There has been a great deal of work on the fall of an isolated particle through a viscous fluid, as well as on the sedimentation of a uniform suspension, but the relative motion between neighbouring particles has received much less attention. Several interesting effects have been observed (Jayaweera, Mason & Slack 1964) and explained (Hocking 1964) with the aid of a fairly simple picture of the viscous forces. This approach will be used here to characterize the stability of a long row of falling particles with initially uniform separations.

A single sphere of radius $a$, drifting at a velocity $U$ through a viscous liquid of viscosity $\mu$, experiences a drag force

$$F_D = 6\pi\mu a U. \tag{1}$$

If a second sphere is placed in the flow field of the first, it is swept along, and falls faster that it would alone. The effective drag force on both particles is reduced by the interaction of their flow fields to approximately (Happel & Bremner 1965, ch. 6)

$$F_D = 6\pi\mu a U\{1 - \tfrac{3}{4}(a/d)\}, \tag{2}$$

where $d$ is the separation between the spheres, and $a/d \ll 1$.

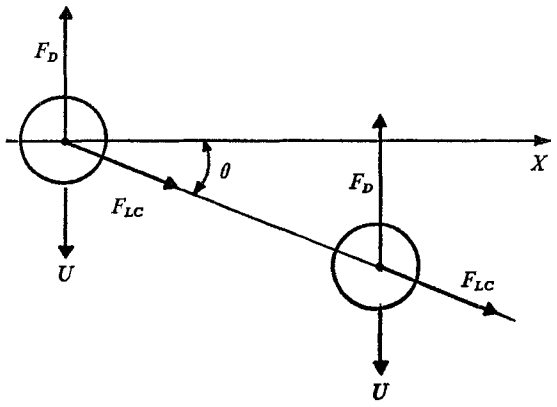


FIGURE 1. Two spherical particles drifting through a viscous liquid.

If the particles are drifting at an angle $\theta$ to the horizontal, an additional force acts along the line of centres,

$$F_{LC} = 6\pi\mu a U\{\tfrac{3}{4}(a/d)\}\sin\theta \tag{3}$$

as sketched in figure 1. The horizontal component of these forces tends to make both spheres glide to one side.

If there are only two particles, the forces on both are equal, and there is no relative motion. The addition of more particles, however, makes relative displacements possible. Consider the configuration of three spheres shown in figure 2 in which the centre sphere is drifting ahead of its two neighbours. All three spheres experience a drag reduction due to their interaction with their neighbours, but this reduction is larger for the centre sphere, since it has two neighbours. As a result, it falls faster, and tends to move ahead of its neighbours.

If the particles are taken two at a time, the glide forces are identical for each

pair, but their resultant on the centre sphere has no lateral component. This causes the leading sphere to fall vertically, while its neighbours glide over to it. The net effect of all these forces is to form a cluster of particles in the wake of the leading particle, leaving open channels where the trailing particles have migrated laterally.

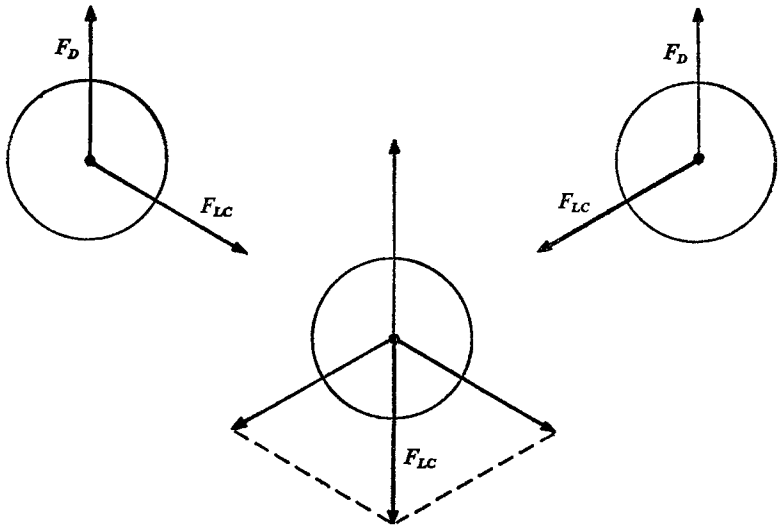


FIGURE 2. Three spherical particles drifting through a viscous liquid.

## 2. Theory

In order to model the interactions which occur when a long row of solid particles drifts through a viscous liquid, we will consider an infinitely long row of identical spheres of radius $a$ distributed (with constant spacing) along a straight line. As a result of an externally applied force, such as gravity or an electric field, the particles drift at right angles to their line of centres with a velocity $U$. Under these conditions, the forces on all the particles are identical, so that the particles maintain their configuration.

If any particle is given a small perturbation (figure 3) from this equilibrium, however, it will experience a net force which may drive the particle even farther from equilibrium, and lead to instability and breakup of the entire layer. If the particles are not too close together ($a/d \ll 1$) this force may be approximated by summing the forces which would act on the particle as a result of its interaction with its two nearest neighbours. This perturbation force consists of two components: a drag component which is anti-parallel to the drift velocity, and a lateral force which leads to clustering of the particles.

The drag force on the $n$th sphere may be obtained by summing the forces exerted by its two nearest neighbours:

$$(F_D)_n = 6\pi\mu a U\left[1-\frac{3}{4}\left(\frac{a}{d+(\xi_{n+1}-\xi_n)}+\frac{a}{d+(\xi_n-\xi_{n-1})}\right)\right], \tag{4}$$

where $\xi$ is the horizontal displacement of the sphere from its equilibrium position.

When $\xi$ is very small, the perturbation force may be approximated as

$$6\pi\mu aU(\tfrac{3}{4}a/d^2)(\xi_{n+1}-\xi_{n-1}).$$

Note that this perturbation force does not depend on the position of the $n$th particle, but only on the net separation between its two neighbours.

The force along the line of centres appears only when neighbouring particles have different vertical positions. For small vertical displacements ($\eta$) of neighbouring particles

$$\sin\theta \simeq (\eta_{n+1}-\eta_n)/d$$

and the perturbed line-of-centres force acts in the horizontal direction with a magnitude

$$F_{LC} = 6\pi\mu aU(\tfrac{3}{4}a/d^2)(\eta_{n+1}-\eta_{n-1}). \tag{5}$$

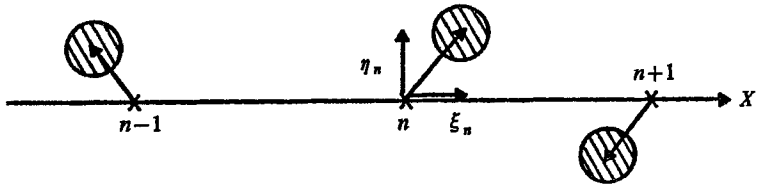


FIGURE 3. Perturbations in the originally uniform row of particles.

Equations of motion for the perturbed position of the $n$th sphere are obtained by equating the drag force on the sphere to the viscous forces due to interactions with its nearest neighbours:

$$\partial\eta_n/\partial t = -\alpha[\xi_{n+1}-\xi_{n-1}], \tag{6}$$

$$\partial\xi_n/\partial t = \alpha[\eta_{n+1}-\eta_{n-1}], \tag{7}$$

where

$$\alpha = \tfrac{3}{4}(a/d)(U/d). \tag{8}$$

For an infinite array of particles, these equations have solutions of the form

$$\xi_n, \eta_n \propto e^{\beta t}e^{jknd},$$

where $k$ is the wave-number of the perturbation. Substitution of this expression into (6), (7) gives a relation between the growth rate and wave-number which must be satisfied for a solution, namely

$$\beta^2 = 4\alpha^2\sin^2(kd). \tag{9}$$

This condition is the dispersion relation for perturbations of the particle positions. To determine whether the initial equilibrium is stable, we must examine the time dependence of the perturbations for all allowed real values of wave-number $k$. Because the system is periodic, there are limits to real values of $k$ which correspond to physically meaningful solutions. The shortest allowed wavelength, which occurs when alternate particles move in opposite directions, is $\lambda_{\min} = 2d$, corresponding to a maximum allowed wave-number of

$$k_{\max} = \frac{2\pi}{\lambda_{\min}} = \frac{\pi}{d}. \tag{10}$$

The solution of the dispersion relation (9),

$$\beta = \pm 2\alpha \sin(kd),$$

is plotted in figure 4 over the allowed range

$$0 \leqslant kd \leqslant \pi.$$

There are two branches to the dispersion relation. In one branch, $\beta$ is always positive, while in the other $\beta$ is negative. Since the perturbation is proportional to $e^{\beta t}$, that mode with positive $\beta$ will grow exponentially in time, indicating instability for all allowed wave-numbers. The mode with negative $\beta$, on the other hand, is stable because it decays with time.

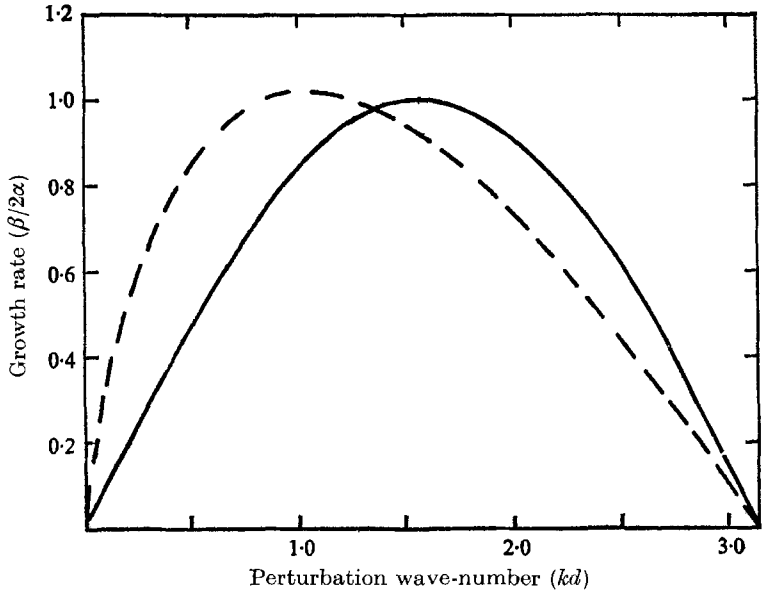


FIGURE 4. The growth rate of the viscous instability as a function of the wave-number of the disturbance. —, nearest-neighbour theory; - - -, theory with all neighbours.

The most unstable mode ($\beta = +2d$), which occurs at $kd = \frac{1}{2}\pi$, has four particles in each wavelength. The appearance of this mode can be deduced from the equations of motion and the dispersion relation. If the vertical disturbance at maximum instability is given by

$$\eta_0 \cos(\tfrac{1}{2}n\pi) e^{2\alpha t}, \tag{11}$$

then substitution into the equations of motion gives the horizontal disturbance as

$$\xi = -\eta_0 \sin(\tfrac{1}{2}n\pi) e^{2\alpha t}. \tag{12}$$

The particle displacements and velocities implied by these equations are sketched in figure 5. The leading particle tends to fall faster as its two neighbours approach it, while the trailing particles in the centre of a widening channel tend to fall more slowly. As the perturbation grows, the leading particle and its two neighbours form a clump which falls through the liquid, leaving every fourth particle behind. Thus, an initially uniform layer of particles will not remain uniform when drifting

through a viscous liquid. Any small irregularity will be amplified by the viscous forces, and eventually the entire layer will break up into clumps of several particles, separated by clear channels. The breakup will not usually be as regular as that discussed here but, since all possible wavelengths are unstable, the breakup will always occur with the clumps and channels containing varying numbers of particles.

The stable mode ($\beta = -2\alpha$) which occurs at this wave-number is also shown in figure 5. In this case, the leading particle finds itself in the centre of a wide gap, and therefore falls slower, while the trailing particle catches up. Thus, this mode tends to return to the equilibrium position, as expected from the solution of the dispersion relation.

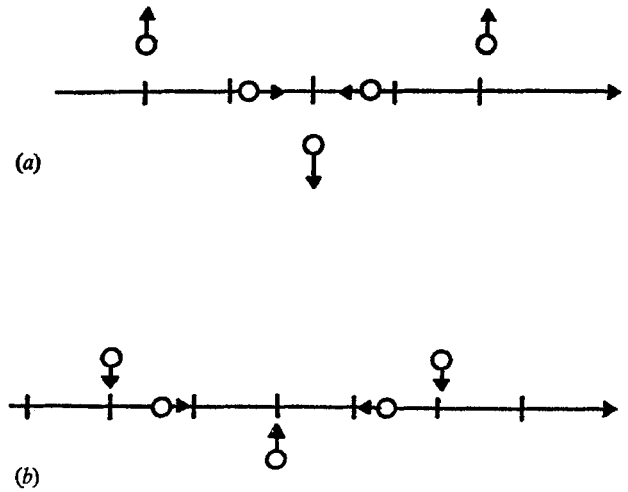


FIGURE 5. Motion of the particles in the stable and unstable modes corresponding to $\lambda = 4d$. (*a*) Unstable mode. (*b*) Stable mode.

So far, the analysis has only considered the force on the $n$th sphere due to its interaction with its nearest neighbours. It is not difficult to extend the results to the more realistic case in which the $n$th particle is influenced by all of the other particles on either side, since the additional forces can be added, due to the linearity of the creeping flow equations and the assumption $a/d \ll 1$ (Hocking 1964). The derivation of the equations of motion follows, as before, with the first equation given by

$$6\pi\mu aU\partial\eta_n/\partial t = 6\pi\mu aU(3a/4d^2)\times\{(\xi_{n+1}-\xi_{n-1})+(1/2^2)(\xi_{n+2}-\xi_{n-2})+\ldots + (1/l^2)(\xi_{n+l}-\xi_{n-l})+\ldots\}. \quad (13)$$

The only change is the addition of extra terms corresponding to the additional interactions with particles at greater distances. These terms contain the factor $l^{-2}$, indicating that the force falls off as the inverse square of the separation.

The second equation of motion is similarly modified, and the dispersion relation becomes

$$\beta^2 = 4\alpha^2 \sum_{l=1}^{\infty} \frac{\sin l(kd)}{l^2}. \quad (14)$$

The solution of this dispersion relation for allowed values of $kd$ is plotted in figure 4. The most unstable mode is shifted to longer wavelengths, but the maximum growth rate is only slightly affected.

So far, the growth rate has been discussed in terms of time. Since the particle layer is falling with the average velocity $U$, any elapsed time is equivalent to a distance

$$z = Ut$$

and the disturbance, therefore, grows as

$$e^{\beta t} = e^{\beta z/U} \equiv e^{\gamma z}.$$

The spatial growth rate,

$$\gamma = \tfrac{3}{2}a/d^2, \tag{15}$$

depends only on the geometry of the layer. Since the spatial growth is independent of particle velocity, the disturbance of a given layer will be amplified the same amount when it falls a given distance, no matter how fast it may be falling. The breakup of the layer cannot be modified by changing the drift velocity, but only by changing the geometry.

## 3. Experiments

In order to test this theory, several experiments were performed by dropping steel balls through Venice turpentine, whose viscosity was measured as approximately $10^4$ poise. Since the Reynolds number of the $\frac{1}{16}$ in. balls used in the experiment was less than $10^{-6}$, the Stokes approximation should be valid.

The experiment was conducted in a glass box, 4 in. on each side. For each separation distance, $d$, a plastic template was made by drilling $\frac{1}{16}$ in. holes equally spaced along a straight line. The holes were filled with the liquid used, and a steel ball placed in the bottom of each hole. The template containing the balls was then positioned slightly below the surface of the liquid. By inserting a rod of diameter slightly less than $\frac{1}{16}$ in. into a hole, the ball and the liquid above it were forced out into the bulk of the liquid, where the ball began to fall under gravity. Starting the ball slightly below the surface in this manner eliminated the tendency to stick to the rod or template, as well as preventing a variable delay in penetrating the liquid surface.

When the balls were started uniformly, the clumping and channelling predicted by the theory occurred irregularly. To compare the experiment and the theory, it was found more convenient to impose an initial perturbation on the particles, and to follow its growth as the particles fell. Since it is difficult to vary the horizontal spacing in the template, but relatively easy to vary the vertical position by releasing the balls at different times, the initial perturbation used here had only a vertical component. Pictures of the falling spheres released in this manner were taken with both multiple and single exposures.

The qualitative aspects of the predicted instability are immediately apparent from these pictures. In the multiple exposure of figure 6 (plate 1), the widening channels containing a single particle are clearly visible, while in the single exposure of an advanced stage of the instability (figure 7, plate 1) the clumping into groups of three is quite striking.

The quantitative growth of the disturbance can also be determined from these pictures, but, since the initial configuration does not correspond to one of the normal modes discussed in the previous section, the disturbance will not grow as a simple exponential. The behaviour to be expected can be determined by solving the equations of motion with the boundary conditions implied by the experiment:

$$\xi_n(t=0) = 0,$$

$$\eta_n(t=0) = \eta_0 \cos(nkd).$$

Combination of the two normal modes to satisfy this condition gives

$$\eta = \eta_0 \cos(nkd) \cosh(\gamma z), \tag{16}$$

$$\xi = \eta_0 \sin(nkd) \sinh(\gamma z). \tag{17}$$

In the initial phases of the instability, when $\gamma z$ is small, the vertical amplitude of the disturbance is approximately constant:

$$\eta \simeq \eta_0 \cos(nkd),$$

while the horizontal amplitude grows linearly:

$$\xi \simeq \eta_0(\gamma z) \sin(nkd).$$

Since the horizontal and vertical amplitudes, as well as $z$, can be measured directly from the photographs, the spatial growth rate $\gamma$ can be determined from

$$\gamma = \frac{1}{z} \frac{\text{amplitude of } \xi}{\text{amplitude of } \eta} \tag{18}$$

if the measurements are restricted to the initial phases of growth.

The growth rate was determined in this manner by taking the multiple exposures of the falling balls at roughly 2 min intervals at various initial spacings ranging from $\frac{1}{8}$ in. to $\frac{5}{16}$ in. ($\frac{1}{4} \leqslant a/d \leqslant \frac{1}{10}$). Growth rates for perturbations with a wave-number of $k = \pi/2d$, corresponding to the modes sketched in figure 5, were determined. Since the walls affected the fall velocity as well as the growth of the perturbation, measurements were taken only for the channels and clumps developing in the centre of the row.

For each value of spacing, the vertical amplitude of the disturbance was measured from a photograph similar to figure 6. The growth of the horizontal component of the disturbances was then obtained from two separate measurements. One measurement was made of the widths of the channels at various depths, giving an increasing amplitude. Another measurement was made of the widths of the clusters which decrease as the spheres fall. In all cases, the growth rate for the clusters was less than that for the channels, indicating that the instability grows more slowly as the particles approach one another. The growth rates for channels and clusters are plotted as a function of $a/d$ in figure 8, along with the prediction of the nearest-neighbour theory. (The correction for additional neighbours, a factor of 0·916, is less than the scatter of the data.) The measured growth rates exhibit the same trend as the theoretical predictions with the magnitude in all cases somewhat less than expected. This decrease in growth rate may be due to the relatively large amplitude needed to observe the instability.

## 4. Conclusion

The experiments described above indicate that the viscous instability predicted by the simple theory of § 2 actually does occur, and that its spatial growth is approximated by $e^{\gamma z}$, where

$$\gamma = \tfrac{3}{2}a/d^2.$$

This result implies that any initial irregularity in a uniform particle distribution will be amplified by viscous forces alone. Significant amplification will occur when the particle has drifted a small multiple of the separation distance, if this separation is not much greater than the particle diameter. Thus, any initially uniform particle layer will form clusters as it drifts through a viscous fluid. The

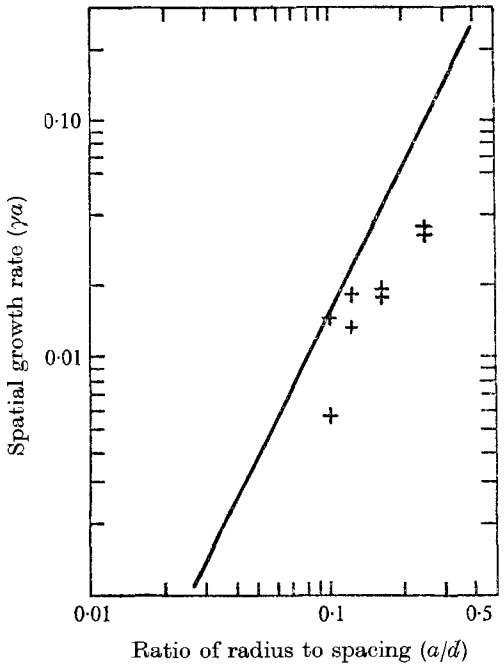


FIGURE 8. The growth rate of the viscous instability for $\lambda = 4d$, as determined by: —, nearest-neighbour theory; +, experiment.

distance in which this clustering occurs will be unaffected by changes in the particle velocity, as long as the Reynolds number remains small. The preferred form of irregularity will consist of small clusters separated by individual particles which trail some distance behind.

I would like to thank Thomas McMullen for his assistance in the construction of the apparatus.

REFERENCES

CROWLEY, J. M. 1967 *Phys. Fluids*, **11**, 1372.

JAYAWEERA, K. O. L. F., MASON, B. J. & SLACK, G. W. 1964 *J. Fluid Mech.* **20**, 121.

HAPPEL, J. & BRENNER, H. 1965 *Low Reynolds Number Hydrodynamics*. Prentice-Hall.

HOCKING, L. M. 1964 *J. Fluid Mech.* **20**, 129.

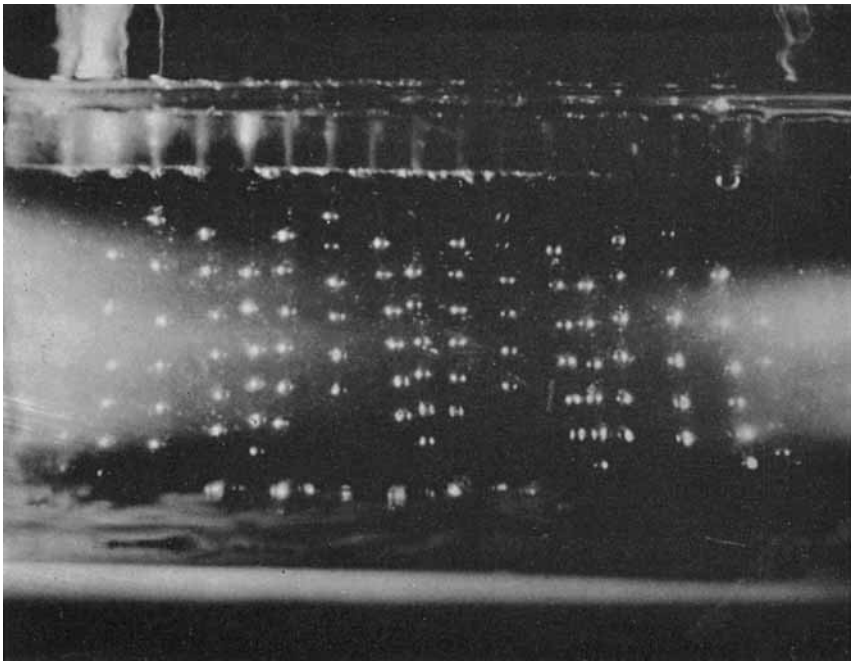

FIGURE 6. A multiple exposure photograph of a falling row of spheres, showing the formation of channels.

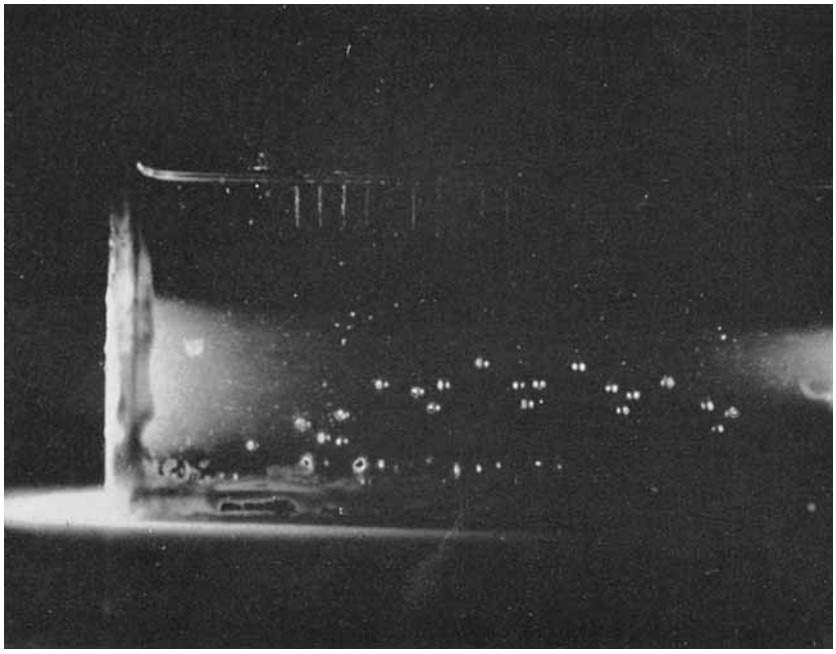

FIGURE 7. A single exposure photograph of an advanced stage of the instability, showing the triplet clusters, and the trailing particles.